An Investigation of the Electronic Structure of Bis(η^5-cyclopentadienyl) Dicarbonyl Complexes of Titanium(II) and Zirconium(II). Discrete Variational Xα Calculation and Gas-Phase Photoelectron Spectroscopy

Maurizio Casarin

Istituto di Chimica dell'Università della Basilicata, 85100 Potenza, Italy

Enrico Ciliberto, Antonino Gulino, and Ignazio Fragalà*

Dipartimento di Scienze Chimiche, Università di Catania, 95125 Catania, Italy

The electronic structure of the unique group IVB metal carbonyls $M(Cp)_2(CO)_2$ has been studied by using the SCF Hartree–Fock–Slater first-principle discrete variational Xα method. Theoretical results nicely fit both experimental ionization energies and relative intensity data taken from He I versus He II photoelectron spectra. Furthermore, they provide an accurate description of the M–CO bonding that appears strongly dominated by π-back-bonding interactions. No evidence has been found either of σ or π donation in accordance with other physicochemical data. The back-donation to π^* carbonyl orbitals mainly involves the metal-based HOMO, and the values of the clearly resolved vibrational interval associated with ionization from this orbital provide experimental support for these theoretical findings. The intriguing HOMO–LUMO relationships might be of relevance to explain reactivities and substitution kinetic data of the complexes.

Introduction

The group IVB divalent element organometallics represent an area of expanding interest. Very few examples of such compounds are yet known.[1,2] Nevertheless, they possess an intriguing chemistry mostly related to their carbene-like properties.[2] In this context $M(\eta^5\text{-}C_5H_5)_2(CO)_2$ complexes [hereafter $M(Cp)_2(CO)_2$] are particularly attractive. They are rare examples of group IVB carbonyls that suffer oxidative addition[3] and react with a large variety of electrophilic substrates[4] through reactions that can be formally considered as insertion into various covalent bonds[5] or addition to multiple bonds of the carbene-like unit $M(Cp)_2$.[4c,6] Such a reactivity correlates with their high catalytic activity in the hydrogenation of olefins and acetylenes under mild conditions.[2b,7] In this context, the ability of the Zr(II) complex to form rather unusual transoid structures with conjugated dienes[8] is worthy of note.

Moreover accurate studies on the carbonyl substitution kinetics of a large series of titanium–triad complexes have carefully documented that these early-transition low-valent metal systems prefer π-acid rather than σ-bonded ligands.[9] Similarly thermodynamic data on the M–CO bond disruption enthalpy of the present Ti(II) complex[10] have revealed significant differences with respect to those of other π-acid ligands.

This chemistry must necessarily be related to electronic prerequisites that provide a suitable pattern of HOMOs and LUMOs, thus governing the intriguing relationships between the thermodynamic stabilities and the kinetic labilities of the group IVB carbonyls.

Finally, it is worth remembering the large interest currently attached to Ti(0) 18-electron carbonyls.[11] Therefore, there was enough motivation for us to expand our previous study on $Ti(Cp)_2(CO)_2$[12] to a more extensive investigation of the electronic structure of $M(Cp)_2(CO)_2$ (M = Ti, Zr) complexes that involve both combined He I/He II gas-phase UV photoelectron (PES) spectroscopy and first-principle SCF Hartree–Fock–Slater discrete variational (DV) Xα calculation.

Experimental Section

$Zr(Cp)_2(CO)_2$ has been synthesized according to published procedures.[1e] High-resolution PE spectra have been accumulated

(1) (a) Gell, K. I.; Schwartz, J. *J. Am. Chem. Soc.* **1981**, *103*, 2687–2695. (b) Fachinetti, G.; Floriani, C.; Marchetti, F.; Mellini, M. *J. Chem. Soc., Dalton Trans.* **1978**, 1398–1403. (c) Bercaw, J. E.; Brintzinger, H. H. *J. Am. Chem. Soc.* **1971**, *93*, 2045–2046. (d) Marvich, R. H.; Brintzinger, H. H. *J. Am. Chem. Soc.* **1971**, *93*, 2046–2048. (e) Thomas, J. L.; Brown, K. T. *J. Organomet. Chem.* **1976**, *111*, 297–301. (f) Fochi, G.; Guidi, G.; Floriani, C. *J. Chem. Soc., Dalton Trans.* **1984**, 1253–1256. (g) Blenkers, J.; Hessen, B.; van Bolhuis, F.; Wagner, A. J.; Teuben J. H. *Organometallics* **1987**, *6*, 459–469. (h) Cardin, D. J.; Lappert, M. F.; Raston, C. L.; Raley, P. I. In *Comprehensive Organometallic Chemistry*; Wilkinson, G.; Stone, F. G. A.; Abel, E. W., Eds.; Pergamon: Oxford, 1982; Vol. 3, Chapter 23.

(2) (a) Barger, P. T.; Santarsiero, B. D.; Armantrout, J.; Bercaw, J. E. *J. Am. Chem. Soc.* **1984**, *106*, 5178–5186. (b) Bercaw, J. E.; Marvich, R. H.; Bell, L. G.; Brintzinger, H. H. *J. Am. Chem. Soc.* **1972**, *94*, 1219–1238.

(3) (a) Floriani, C.; Fachinetti, G. *J. Chem. Soc., Dalton Trans.* **1972**, 790–791. (b) Fachinetti, G.; Floriani, C. *J. Chem. Soc., Dalton Trans.* **1974**, 2433–2436. (c) Sikora, D. J.; Rausch, M. D. *J. Organomet. Chem.* **1984**, *267*, 21–37.

(4) (a) Floriani, C.; Fachinetti, G. *J. Chem. Soc., Dalton Trans.* **1973**, 1954–1957. (b) Chen, T. L.; Chan, T. H.; Shaver, A. *J. Organomet. Chem.* **1984**, *268*, C1–C6. (c) Fachinetti, G.; Floriani, C.; Stoeckli-Evans, H. *J. Chem. Soc., Dalton Trans.* **1977**, 2297–2302. (d) Bercaw, J. E. *J. Am. Chem. Soc.* **1974**, *96*, 5087.

(5) Calderazzo, F. *Angew. Chem.* **1977**, *16*, 299–311.

(6) Gambarotta, S.; Floriani, C.; Chiesi-Villa, A.; Guastini, C. *J. Am. Chem. Soc.* **1982**, *104*, 1918–1924.

(7) Demerseman, B.; Dixneuf, P. H. *J. Chem. Soc., Chem. Commun.* **1981**, 665–666.

(8) (a) Erker, G.; Wicher, J.; Rosenfeldt, K. E. F.; Dietrich, W.; Kruger, C. *J. Am. Chem. Soc.* **1980**, *102*, 6344–6346. (b) Kay, Y.; Kanehisa, N.; Miki, K.; Kasai, N.; Mashima, K.; Nagasuna, K.; Yasuda, H.; Nakamura, A. *J. Chem. Soc., Chem. Commun.* **1982**, 191–192. (c) Tatsumi, K.; Yasuda, H.; Nakamura, A. *Isr. J. Chem.* **1983**, *23*, 145–150. (d) Erker, G.; Engel, K.; Korek, U.; Czisch, P.; Berke, H.; Caubere, P.; Vanderesse, R. *Organometallics* **1985**, *4*, 1531–1536.

(9) Palmer, G. T.; Basolo, F.; Kool, L. B.; Rausch, M. D. *J. Am. Chem. Soc.* **1986**, *108*, 4417–4422.

(10) Dias, A. R.; Dias, P. B.; Diogo, H. P.; Galvao, A. M.; Minas da Piedade, M. E.; Simoes, J. A. M. *Organometallics* **1987**, *6*, 1425–1432.

(11) (a) Kelsey, B. A.; Ellis, J. E. *J. Am. Chem. Soc.* **1986**, *108*, 1344–1345. (b) Kelsey, B. A.; Ellis, J. E. *J. Chem. Soc., Chem. Commun.* **1986**, 331–332. (c) Gardner, T. G.; Girolami, G. S. *Organometallics* **1987**, *6*, 2551–2556. (d) Ming Chi, K.; Frerichs, S. R.; Stein, B. K.; Blackburn, D. W.; Ellis, J. E. *J. Am. Chem. Soc.* **1988**, *110*, 163–171.

(12) Fragalà, I.; Ciliberto, E.; Thomas, J. L. *J. Organomet. Chem.* **1979**, *175*, C25–C27.

by directly interfacing an IBM PC XT computer to the PE spectrometer equipped with a He I/He II (Helectros Development) source. Resolution measured on the He $1s^{-1}$ line was always around 20 meV. The He II spectra were corrected only for the He $II\beta$ "satellite" contributions (10% on reference N_2 spectrum). The spectra were deconvoluted by fitting the spectral profiles with a series of asymmetrical Gaussian envelopes after subtraction of the background. The agreement factors, $R = [\sum(F_o - F_c)^2/\sum(F_o)^2]^{1/2}$, after minimization of the function $\sum(F_o - F_c)^2$ converged to R values of ≤ 0.035. The area of bands thus evaluated was corrected for the analyzer transmission function. PE data on $Ti(Cp)_2(CO)_2$ were taken from our previous work.[12]

Computational Details

Quantum mechanical calculations have been run within the DV-Xα scheme.[13] The molecular electron density was approximated with an s-wave expansion to evaluate the coulomb potential, and the SCF equations were converged by using a self-consistent charge (SCC) procedure[13] which has been found to give good results for molecules containing 3d and 4d atomic orbitals (AOs).[14] Numerical AOs (through 4p on Ti, 5p on Zr, 2p on C, and 1s on H) were used as basis functions. A frozen core approximation (1s, ..., 3p on Ti, 1s, ..., 4p on Zr, 1s on C) has been used throughout the calculations. The ionization energies have been evaluated within the Slater transition-state formalism[15] (TSIEs) to account for reorganization effects upon ionization. For a better understanding of the theoretical data, contour plots (CPs) of some selected molecular orbitals (MOs) have also been analyzed. Geometrical parameters of present complexes were taken from published X-ray data.[16] In the case of the Zr complex, theoretical calculations have been made adopting both the true C_s and an ideal C_{2v} configuration. All the molecular calculations were carried out by running the DV-Xα code in a Vax-11/750 minicomputer.

Results and Discussion

A qualitative description of the bonding in $M(Cp)_2(CO)_2$ molecules can be simply proposed in terms of interactions between relevant valence orbitals of the simpler constituent fragments $M(Cp)_2$ and $(CO)_2$. The electronic structure of the diamagnetic[17] C_{2v} $M(Cp)_2$ fragment can be worked out by evaluating the effects of bending upon a metallocene-like structure of D_{5h} symmetry.[18] This causes the energy splitting of degenerate levels (Figure 1).

A major effect must be associated to metal-based e_2' orbitals that give the destabilized C_{2v} levels $3a_1$ and $3b_2$ mainly because of the increased σ antibonding as one departs from the θ = 180° geometry.[19] A similarly pronounced energy rise will be associated with the a_1' (D_{5h}) level because both of the mixing, in the lower symmetry, with the more internal metal-based $3a_1$ orbital and of a better overlap with the metal d_{z^2} orbital in the bent con-
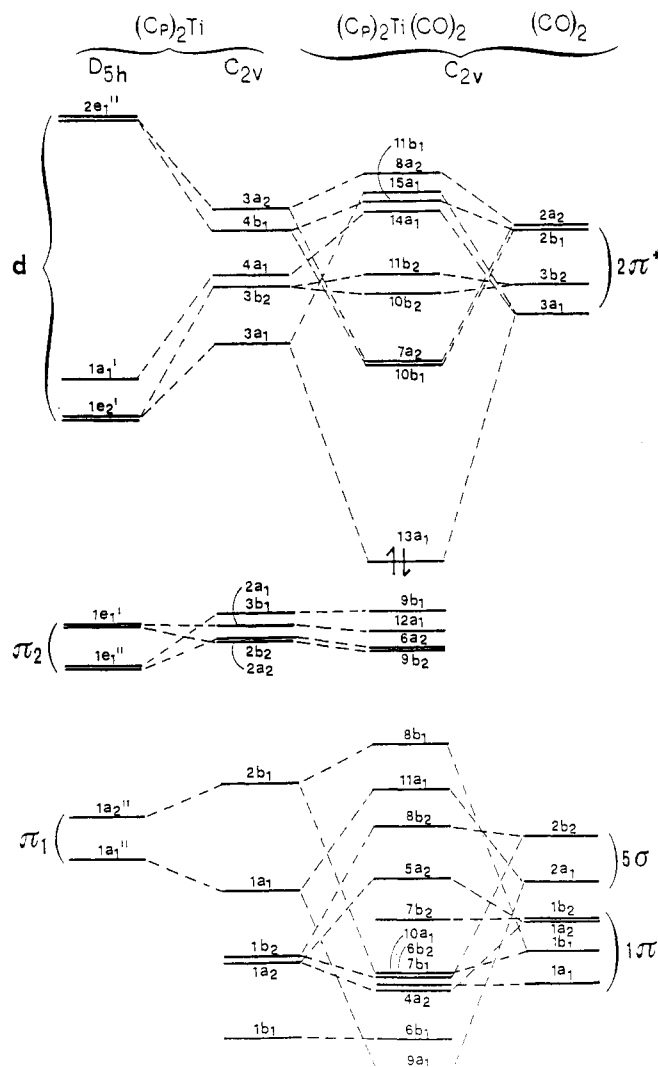

Figure 1. Formation diagram of $Ti(Cp)_2(CO)_2$ involving ground-state eigenvalues of $M(Cp)_2$ and $(CO)_2$ fragments. The energy scale from $8b_1$ through $9a_1$ MOs is three times enlarged in order to give a better understanding of the interactions.

figuration. It is worthy of note, however, that $3a_1$ and $3b_2$ (C_{2v}) orbitals remain dominated by the metal contribution even in the lower C_{2v} symmetry since they relate to nonbonding e_2' orbitals in the D_{5h} MCp_2 fragment. By contrast, a greater admixture with the metal d_{z^2}, $d_{x^2-y^2}$ orbitals will be observed in the $4a_1$ orbital because of the abovementioned better overlap. Finally, the e_1''-related orbitals $4b_1$ and $3a_2$ undergo an energy stabilization because of smaller antibonding interactions. The relevant MOs of the $(CO)_2$ cluster in C_{2v} symmetry are, of course, related to $2\pi^*$, 5σ, and 1π carbonyl orbitals[20] and consist (Figure 1) of pairs of in-phase and out-of-phase linear combinations of the same orbitals (IPLC and OPLC respectively). According to simple Hückel considerations, 5σ and $2\pi^*$ CO combinations may provide remarkable interactions respectively with the $4a_1$, $3b_2$, and $3a_1$ fragment orbitals.[18] In reality, however, such a simplified model, which is based upon simple overlap consideration, may show remarkable limitations either because of the large energy separation between filled CO combinations and metal-based MCp_2 orbitals or because of alternative interactions, allowed in the

(13) (a) Averill, F. W.; Ellis, D. E. *J. Chem. Phys.* **1973**, *59*, 6411–6418. (b) Rosen, A.; Ellis, D. E.; Adachi, H.; Averill, F. W. *J. Chem. Phys.* **1976**, *65*, 3629–3634 and references therein. (c) Trogler, W. C.; Ellis, D. E.; Bekowitz, J. *J. Am. Chem. Soc.* **1979**, *101*, 5896–5901.

(14) (a) Bursten, B. E.; Casarin, M.; Ellis, D. E.; Fragalà, I.; Marks, T. J. *Inorg. Chem.* **1986**, *25*, 1257–1261. (b) Ellis, D. E. In *Actinides in Perspective*; Edelstein, N. M., Ed.; Pergamon: Oxford, 1982, p 123.

(15) Slater, J. C. *Quantum Theory of Molecules and Solids. The Self-Consistent Field for molecules and Solids*; McGraw-Hill: New York, 1974; Vol. 4.

(16) (a) Atwood, J. L.; Stone, K. E.; Alt, H. G.; Hrncir, D. C.; Rausch, M. D. *J. Organomet. Chem.* **1975**, *96*, C4–C6. (b) Atwood, J. L.; Rogers, R. D.; Hunter, W. E.; Floriani, C.; Fachinetti, G.; Chiesi-Villa, A. *Inorg. Chem.* **1980**, *19*, 3812–3817.

(17) Wailes, P. C.; Coutts, R. S. P.; Weigold, H. *Organometallic Chemistry of Titanium, Zirconium and Hafnium*; Academic: New York, 1974.

(18) Lauher, J. W.; Hoffmann, R. *J. Am. Chem. Soc.* **1976**, *98*, 1729–1742.

(19) Similarly, differential improving of metal–ligand overlaps must be responsible for the energy sequence associated with Cp-based $1e_1''$ and $1e_1'$ orbitals in the bent conformation.

(20) In C_{2v} symmetry, the degeneracy of π orbitals is necessarily removed. Therefore, the resulting orbitals are better described in terms of $\pi_{\parallel}$ and $\pi_{\perp}$ orbitals defined by reference to the plane containing the $M(CO)_2$ fragment.

Table I. Orbitals, Eigenvalues, and Population Analysis of Ti(Cp)₂(CO)₂

MO	eV			Ti			2Cp	2CO	character
	GS	TSIE	IE[a]	4s	4p	3d			
13a₁	4.51	7.24	6.35	0	1	53	8	38	d → π*∥(CO)[b]
9b₁	6.58	9.00		0	0	14	78	8	
12a₁	6.80	9.23	9.15	0	0	11	88	1	π₂
6a₂	6.98	9.33		0	0	12	82	6	
9b₂	7.00	9.34		0	0	7	90	3	
8b₁	9.49	11.84		0	0	1	81	18	π₁
11a₁	9.64	11.98		0	0	2	48	50	[5σ(CO) + π₁(Cp)]
8b₂	9.78	12.09	12.67	0	0	4	12	84	5σ(CO)
5a₂	9.97	12.29		0	0	0	36	64	π⊥(CO)[b]
7b₂	10.14	12.69		0	0	1	4	95	π⊥(CO)[b]
6b₂	10.34	12.75	13.19	0	0	0	86	14	σ(Cp)
4a₂	10.38	12.83		0	0	1	65	34	σ(Cp)
7b₁	10.33	12.84		0	0	0	21	79	π⊥(CO)[b]
6b₁	10.56	12.87	13.61	0	0	1	99	0	σ(Cp)
10a₁	10.35	12.88		0	0	0	8	92	π∥(CO)[b]
9a₁	10.64	13.04	14.01	0	0	0	51	49	[5r(CO) + π₁(Cp)]

overlap pop.	overall charge
Ti–C(CO), 0.44	Ti, +1.48
Ti–Cp, 0.113	Cp, –0.42
C–O, 1.20	CO, –0.32

[a] Taken from data in ref 12. [b] ⊥ and ∥ symbols refer to the plane through the metal atom and the carbonyl groups.

Table II. Orbitals, Eigenvalues, and Population Analysis of Zr(Cp)₂(CO)₂

MO	eV			Zr			2Cp	2CO	character
	GS	TSIE	IE[a]	5s	5p	4d			
13a₁	4.34 (4.57)	(7.27)	6.05	0	1	56	8	35	d → π*∥(CO)[b]
9b₂	6.45 (6.69)	(9.09)	8.65	0	1	3	95	1	
12a₁	6.80 (6.98)	(9.32)	8.92	0	0	5	95	0	π₂
6a₂	7.09 (7.22)	(9.77)	9.14	0	0	17	77	6	
9b₁	6.95 (7.28)	(10.02)	9.51	0	0	14	79	7	
8b₁	9.44 (9.68)	(11.92)		0	0	1	90	9	π₁
11a₁	9.60 (9.84)	(12.04)		0	0	5	61	34	[5σ(CO) + π₁(Cp)]
8b₂	10.06 (10.22)	(12.36)		0	0	4	0	96	5σ(CO)
7b₂	10.15 (10.34)	(12.42)		0	0	2	18	80	π∥(CO)[b]
5a₂	10.32 (10.51)	(12.58)	12.68	0	0	0	12	88	π⊥(CO)[b]
10a₁	10.38 (10.52)	(12.65)		0	0	0	11	89	π∥(CO)[b]
4a₂	10.39 (10.57)	(12.71)		0	0	0	91	9	σ(Cp)
9a₁	10.46 (10.64)	(12.86)		0	0	0	29	71	[5σ(CO) + π₁(Cp)]
7b₁	10.47 (10.71)	(12.92)		0	0	1	10	90	π⊥(CO)[b]

overlap pop.	overall charge
Zr–C(CO), 0.50	Zr, +1.40
Zr–Cp, 0.106	Cp, –0.42
C–O, 1.19	CO, –0.28

[a] IE values are taken from the deconvoluted spectrum. [b] ⊥ and ∥ symbols refer to the plane through the metal atom and the carbonyl groups. Values in parentheses refer to C_s symmetry.

lower symmetry, could be favored due to a better energy matching (Figure 1).

Ground-state (GS) DV-Xα calculations on Ti(Cp)₂(CO)₂ provide an adequate rationale both for the mentioned expectations as well as for questions that emerge from such a qualitative description. Population data (Tables I and II) indicate that the filled MOs are grouped in three well-defined energy ranges, and each group includes MOs which, in terms of a qualitative localized bonding model, reproduce: (i) the metal d filled subshells, (ii) the combination of the upper-filled π_2 MOs, and finally (iii) the Cp innermost π_1, the CO 5σ and 1π, and some internal Cp σ MOs which all lie within a 1-eV range.

These last-mentioned MOs possess almost no metal d contribution. Some of them (11-9a₁ and 5-4a₂) result from nonbonded interligand 5σ–π₁ (Cp) and $\pi_\perp$(CO)–σ(Cp) interactions, respectively, while the remainder are dominated either by the Cp or by the CO character (Tables I and II).

The MOs 9b₁ through 9b₂ obviously correlate with the e₁″ and e₁′ MOs of the D_{5h} M(Cp)₂ fragment. Their par-

Table III. Orbitals, Eigenvalues, and Population Analysis of Ti(Cp)₂(CO)₂ and of Zr(Cp)₂(CO)₂ (Empty Orbitals)

MO	GS, eV	Ti 4s	4p	3d	2Cp	2CO	MO	GS, eV	Zr 5s	5p	4d	2Cp	2CO
10b₁	2.066	0	0	19	33	48	10b₁	2.11	0	3	10	22	65
7a₂	2.05	0	0	19	32	49	7a₂	1.97	0	0	8	25	67
10b₂	1.27	0	3	12	12	73	10b₂	1.40	0	7	15	24	54
11b₂	1.07	0	1	29	39	31	11b₂	0.90	0	0	19	30	51
14a₁	0.42	0	0	44	22	34	14a₁	0.49	0	3	20	32	45
11b₁	0.30	0	0	26	34	40	15a₁	-0.08	2	1	51	27	19
15a₁	0.25	0	1	39	20	40	8a₂	-0.36	0	0	34	66	0
8a₂	0.04	0	0	43	13	44	11b₁	-0.77	0	0	32	43	25
12b₁	-0.47	0	0	24	63	13	9a₂	-0.99	0	0	32	36	32
16a₁	-0.76	3	0	24	69	4	12b₁	-1.12	0	0	24	66	10
9a₂	-1.03	0	0	0	38	62	12b₂	-1.56	0	4	26	57	13
12b₂	-1.15	0	0	26	61	13	16a₁	-1.94	1	0	24	63	12
17a₁	-2.90	13	4	4	79	0	17a₁	-3.35	1	0	3	95	1
13b₁	-4.13	0	3	1	96	0	13b₁	-3.91	0	4	0	96	0
13b₂	-5.42	0	0	0	100	0	18a₁	-4.58	0	0	3	95	2

ticular energy sequence, not dependent upon the CO coordination since the carbonyl contributions to these MOs are of a minor relevance (Tables I,II), is certainly due to differential raising or lowering effects upon bending (Figure 1). Finally, population data and, hence, the contour plots in Figure 2 clearly show that the HOMO 13a₁ is dominated by the metal d and CO contributions because of back-donation of metal d electron density (d_{z^2}, $d_{x^2-y^2}$) into the π* CO orbital (Figure 2a,b).

The virtual MOs that follow are worthy of some comments. Inspection of Table III reveals that the MOs 10b₁ through 16a₁ all possess significant contributions from metal d subshells. Furthermore, contour plot analysis reveals that the ligand contribution is always CO in character and is due to admixture with the π*-related MOs. These observations are in accordance with the qualitative interaction scheme pictured in Figure 1.

Theoretical results for the Zr complex (Table II) are very similar. The most apparent difference consists in a changed energy sequence of e₁″, e₁′-related MOs (Table II) whose pattern becomes strongly reminiscent of that encountered in the case of sandwich metallocenes. This observation is nicely tuned with the wider Cp(centroid)-Zr-Cp(centroid) angle (143.4°) than that in the Ti analogue (138.6°).

TSIE's evaluated for selected outermost MOs are listed in Tables I and II. As expected, reorganization effects in the ion states are greater for MOs having larger metal d contributions even though differential values are not always large enough to upset the GS energy sequence. Accordingly, the assignments of the PE spectra[21] (Figure 3a,b) become a straightforward matter (Tables I and II).

There is no doubt that the onset band represents the ionization from the 13a₁ orbital. The band in both cases increases in relative intensity (Tables IV) upon switching to the He II radiation, and this behavior is certainly peculiar to MOs having significant metal d contributions.[22] The band envelope that follows between 8 and 10 eV must be assigned to ionization of Cp MOs. In the case of Ti-(Cp)₂(CO)₂,[12] the band is structureless, thus precluding any detailed assignment, while it is clearly resolved in three components (Figure 3a) in the complex of the heavier Zr. Such a better resolution finds a nice counterpart in the

Table IV. Relevant PE Data, Computed TSIE's, and Assignments of PE Spectra

Ti(Cp)₂(CO)₂

band[c] label	eV IE	TSIE	rel intens[a] He I	He II	assignt[b]
a	6.35	7.24	0.20	0.50	13a₁
b	9.15	9.00 / 9.23 / 9.33 / 9.34	1.00	1.00	9b₁ / 12a₁ / 6a₂ / 9b₂

Zr(Cp)₂(CO)₂

band label	eV IE	TSIE	rel intens[d] He I	He II	assignt[e]
a	6.05	7.27	0.62	2.82	13a₁
b	8.65	9.09	1.03	1.02	9b₂
b′	8.92	9.32	1.00	1.00	12a₁
b″	9.14	9.77	1.04	1.19	6a₂
b‴	9.51	10.02	1.18	1.42	9b₁

[a] The intensity of band b has been taken as reference. [b] See Table I for dominant characters. [c] See Figure 1 in ref 12. [d] The intensity of band b′ has been taken as reference. [e] See Table II for dominant characters.

wider energy spreading of TSIE values (1 eV against 0.34 eV; Tables I and II). Upon switching to the He II spectrum (Figure 3b), the components b″ and b‴ become more intense (relative to b and b′) (Table IV) in accordance with the greater metal d admixture in corresponding MOs (Table II). The spectral features appearing in the higher IE range up to 10.5 eV show a poor resolution, and, therefore, correlation with GS eigenvalues must be considered qualitatively.

Finally, we comment on structures observed in the higher IE side of metal d⁻¹ ionization (Figure 3c). The intervals measured in the PE spectra (Ti, 2300 ± 150 cm⁻¹;[12] Zr, 2100 ± 150 cm⁻¹) can be compared with the frequency of the CO stretching modes observed in the IR spectra[1e] (1975 and 1897 cm⁻¹ for Ti complex; 1978 and 1888 cm⁻¹ for Zr complex), thus supporting a mechanism that involves excitation of vibrational modes upon ionization. Incidentally, we note that these complexes represent almost unique examples of clearly resolved vibrational progressions associated with a d⁻¹ metal ionization.[23] Of particular relevance are the greater vibrational intervals (with respect to those found in IR spectra) measured in

(21) The assignment is also in tune with a large variety of data on several M(Cp)₂X₂ complexes. See, for example: Green, J. *Struct. Bonding (Berlin)* 1981, *43*, 37–112.

(22) (a) Egdell, R. G.; Orchard, A. F.; Lloyd, D. R.; Richardson, N. V. *J. Electron Spectrosc. Relat. Phenom.* 1977, *12*, 415–423. (b) Egdell, R. G.; Orchard, A. F. *J. Chem. Soc., Faraday Trans. 2* 1978, *74*, 485. (c) Egdell, R. G.; Orchard, A. F. *J. Electron Spectrosc. Relat. Phenom.* 1978, *14*, 277. (d) Egdell, R. C. Ph.D. Thesis, Oxford, 1979.

(23) Less resolved vibrational structures have been detected in PE spectra of other carbonyls. See, for example: (a) Lichtenberger, D. L.; Calabro, D. C.; Kellogg, G. E. *Organometallics* 1984, *3*, 1623–1630. (b) Lichtenberger, D. L.; Kellogg, G. E. *J. Am. Chem. Soc.* 1986, *108*, 2560–2567.
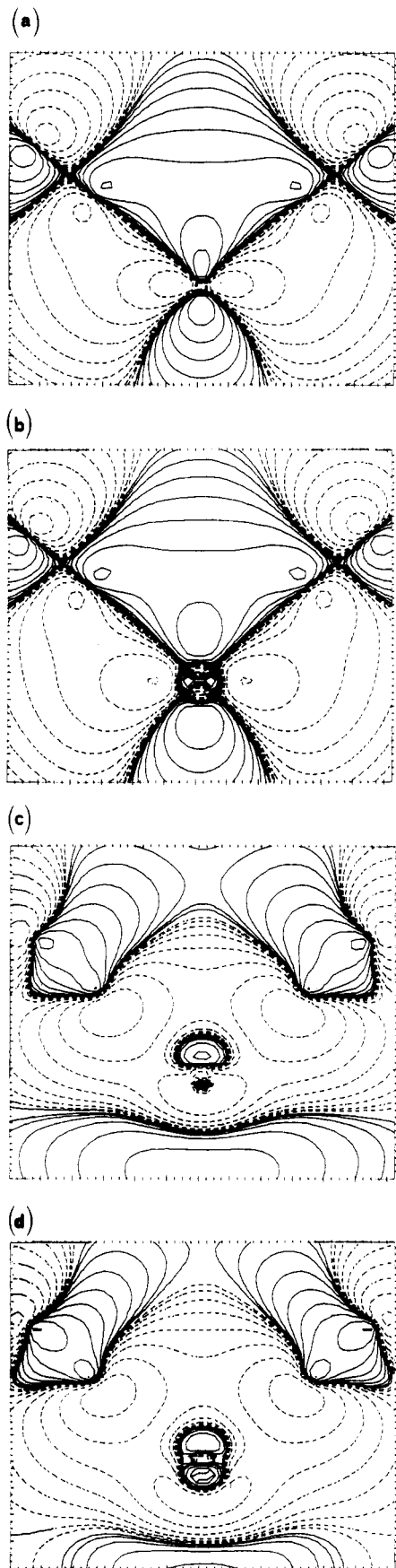
Figure 2. DV-Xα contour plots of $13a_1$ and $11a_1$ MOs of M-$(Cp)_2(CO)_2$ complexes in the yz plane: (a) $13a_1$ (HOMO), M = Ti; (b) $13a_1$ (HOMO), M = Zr; (c) $11a_1$, M = Ti; (d) $11a_1$, M = Zr. The contour values are ±0.0065, ±0.013, ±0.026, ±0.052, ±0.104, ±0.208, ±0.416, and ±0.832 $e^{1/2}/A^{3/2}$. Dashed lines refer to negative values.
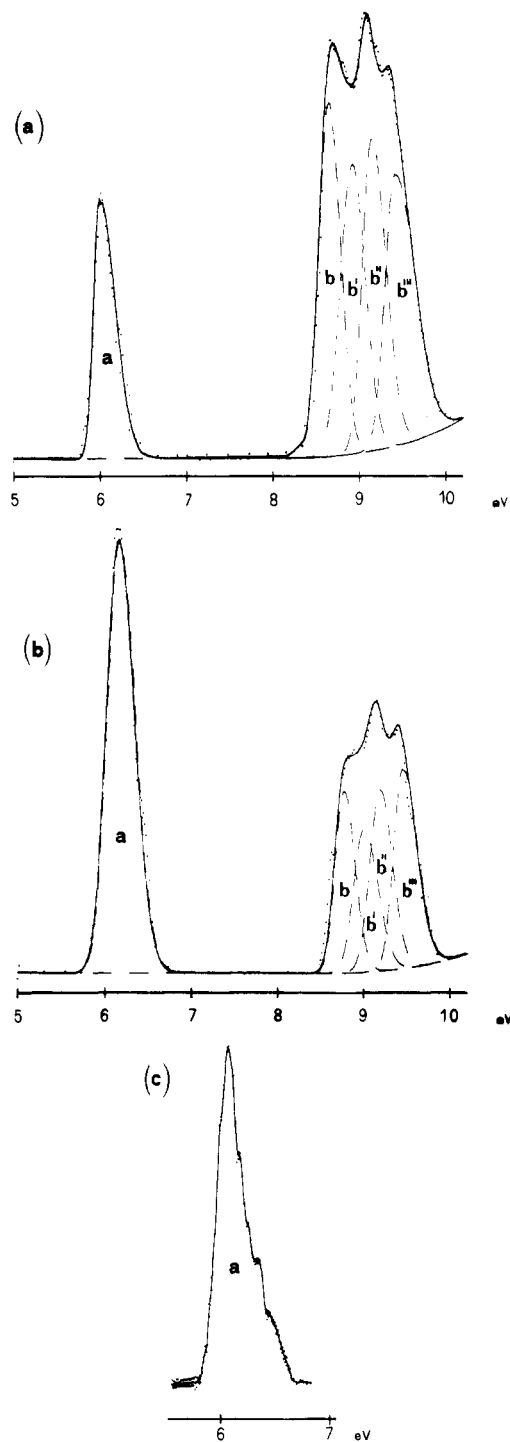
Figure 3. (a) He I photoelectron spectrum of $Zr(Cp)_2(CO)_2$ (5.0–10.2 eV region). (b) He II photoelectron spectrum of Zr-$(Cp)_2(CO)_2$ (5.0–10.2 eV region). (c) Expanded scale of the onset band.

the PE spectra. This observation stresses a back-bonding donation mechanism governing the composition of $13a_1$ MO. As a matter of fact, the removal of d-electron density in the $13a_1^{-1}$ ion state causes a drastic lowering of back-donation in the empty, antibonding π^* CO orbital. Such a mechanism clearly enforces the C=O bonding, shortens the C=O bond length, and, in turn, results in a higher (with respect to IR) frequency of CO stretching vibrational intervals.

Conclusion

The chemistry of low-valent titanium–triad metalloc-

enes-related organometallics is clearly dominated by a strong propensity to reduce the electron density on the metal centers. In simpler metallocenes this tendency appears very well documented both by the ring-hydrogen abstraction[2,24] and by oxidative addition[3] leading to higher valent metal complexes or else by the tendency to saturation of the ligation sphere through coordination of π-acidic ligands.[24] In this context, the CO ligand seems to be particularly effective in stabilizing the $M(Cp)_2$ framework because of its enhanced capability to withdraw electron density via the back-donation mechanism. Similarly, the carbonyl chemistry of the same zerovalent metals[11] appears strongly dependent upon the presence of an ancillary ligand that moves the energy of the metal subshell to values suitable for a strong back-donation.

Even more interesting, the mechanism of CO substitution reactions in $M(Cp)_2(CO)_2$ complexes[1e,9] appears strongly dependent on the nature of the metal centers. Data available today lend support also to the fact that electronic factors govern the observed changes.

Present theoretical data provide, in reality, an adequate rationale to the breadth of such observations. The molecular orbital picture that emerges, once only the filled orbitals are considered, leads one to conclude that the bonded carbonyls would act as a minor perturbation of the $M(Cp)_2$ fragment.

There is only evidence of interligand nonbonded interaction in the $9a_1$ and $11a_1$ MOs. Of course, closer examination of the population data of the HOMO as well as of the virtual MOs that follow provides a clearer indication of the bonding mechanism. It transpires (Figure 1) that the metal-based $M(Cp)_2$ orbitals are all severely admixed with π*-related CO orbitals, thus supporting a M–CO bonding mechanism strongly dominated by back-bonding interactions. The major effect is found associated with orbitals of a_1 symmetry and results in a very remarkable stabilization of the HOMO $13a_1$. Such an effect seems to be the major source of the stability of the present 18-electrons carbonyls since, as already mentioned, there is no evidence of any CO σ and π donation.

These observations are very well-tuned with the abnormally high (with respect to other carbonyls) downfield ^{13}C NMR shift[9] observed in $Zr(Cp)_2(CO)_2$, with the values of IR stretching CO frequencies[25] and, more generally, with the marked propensity of these early-transition low-valent carbonyls to bind π-acid rather than σ-bonded ligands.

Of particular interest is the difference found in the composition of virtual MOs (Table III) on passing from Ti to Zr complexes since those data can be correlated with the differences in their chemistry. In this context we shall make reference to $10b_1$ and $7a_2$, to $14a_1$, and to $15a_1$ and $11b_2$ MOs, respectively, related to e_1'', a_1', and e_2' metal-based $M(Cp)_2$ orbitals. First of all, we note the smaller metal contribution and the predominance of the CO character in the $10b_1$, $7a_2$ orbitals of the $Zr(Cp)_2(CO)_2$. This trend finds a counterpart in the $8a_2$, $11b_1$ pair on passing from the Ti to the Zr complex. Moreover, the energy baricenters of the two pairs of orbitals are clearly greater in the Zr complexes. Such a trend is certainly associated with the wider Cp(centroid)–M–Cp(centroid) angle in $Zr(Cp)_2(CO)_2$, since any conformation approaching a more parallel ring array must necessarily result in a nonbonding character of e_2'- and a_1'-related MOs and in
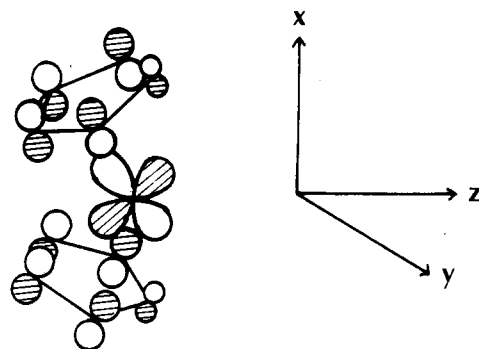

Figure 4. Schematic representation of $4b_1$* metal orbital.

a wider energy separation of e_1''-related MOs.

This peculiarity might be the key to understanding the differences in the substitution mechanism on passing from the Ti to the Zr complex.[9] Kinetic data indicate that the former undergoes dissociation whereas the latter suffers an associative mechanism under the action of nucleophilic phosphines.[9]

In this context we first note that population data (Tables I and II) provide indications that an associative mechanism is much more favorable in the case of the Zr complex because the smaller negative charge on the bonded carbonyls allows more effective dispersion (via back-donation) of the charge brought by the stronger σ-donor phosphine ligand. Furthermore, the associative S_N2 pathway becomes understandable because the $\eta^5 \rightarrow \eta^3 \rightarrow \eta^5$ ring slippage needed to maintain the 18-electron count around the metal seems more favorable in the case of the heavier metal. The ring–allylic coordination[26] required in the mixed carbonyl–phosphine intermediate certainly involves partial population of e_1''-related virtual orbitals. A similar occurrence has been found in $Mo(Cp)_2(NO)R$.[18] The energy of π* phosphine orbitals[27] is likely to result in a better matching with the higher (with respect to the Ti complex) lying e_1''-related orbital[28] and, in turn, in the stabilization of the a'' (π* phosphine orbital) MO which becomes the HOMO in the 20-electron $Zr(Cp)_2(CO)_2(PR_3)$. It is well-known that the e_1'' $M(Cp)_2$ orbitals, in the bent conformation, mix with still higher lying Cp orbitals. Because of the resulting nodal properties (Figure 4), the population of such a HOMO causes asymmetry in the M–Cp bonding and, hence, stabilization of an η^3-allylic ring coordination.

Finally we comment on some relevant details, mainly photoelectron spectroscopic in nature, that emerge from the present investigation. First of all the vibrational structure associated to ionization from the HOMO is worthy of note. To our knowledge, these complexes represent the first case of clearly resolved vibrational excitations associated to ionization of metal-d subshells.[23] This peculiarity is likely to be associated with particularly long-lived ion states. The measured interval provides unambiguous indication of a strong CO character associated with a corresponding MO and, hence, of a remarkable back-bonding mechanism operating at the level of the M–CO bonds. The structures of band associated with Cp ionizations proved to be a sensitive tool for checking the conformation adopted by the ring-sandwich framework.

(24) Brintzinger, H. H.; Bercaw, J. E. *J. Am. Chem. Soc.* **1970**, *92*, 6182–6185.

(25) Busby, R.; Klotzbucher, W.; Ozin, G. A. *Inorg. Chem.* **1977**, *16*, 822–828.

(26) Wong, K. L. T.; Brintzinger, H. H. *J. Am. Chem. Soc.* **1975**, *97*, 5143–5155.

(27) Bursten, B. E.; Darensbourg, D. J.; Kellogg, G. E.; Lichtenberger, D. L. *Inorg. Chem.* **1984**, *23*, 4361–4365.

(28) Note that the mixed $Zr(Cp)_2(CO)_2PR_3$ complex probably belongs to a C_s symmetry. Therefore there are fewer symmetry restrictions than in C_{2v} symmetry.

In particular the pattern observed in the Zr complex, strongly reminiscent of that found in classical metallocenes,[29] witnesses a more parallel array of the two rings. The trend of He I versus He II relative intensity changes

(29) (a) Evans, S.; Green, M. L. H.; Jewitt, B.; Orchard, A. F.; Pygall, C. F. J. Chem. Soc., Faraday Trans. 2 1972, 1847–1865. (b) Evans, S.; Green, M. L. H.; Jewitt, B.; King, G. H.; Orchard, A. F. J. Chem. Soc., Faraday Trans. 2 1973, 356–376.

observed on passing from the Ti to the Zr complex (and incidentally we note the present complexes represent the first case of a group IVB divalent complex studied by PE spectroscopy) provides direct evidence of greater 4d cross section under the higher frequency ionizing radiation, as observed indirectly in earlier studies.[22]
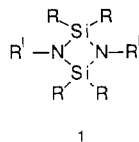
Hydrolysis of Cyclodisilazanes

Robert J. Perry

Corporate Research Laboratories, Eastman Kodak Company, Rochester, New York 14650

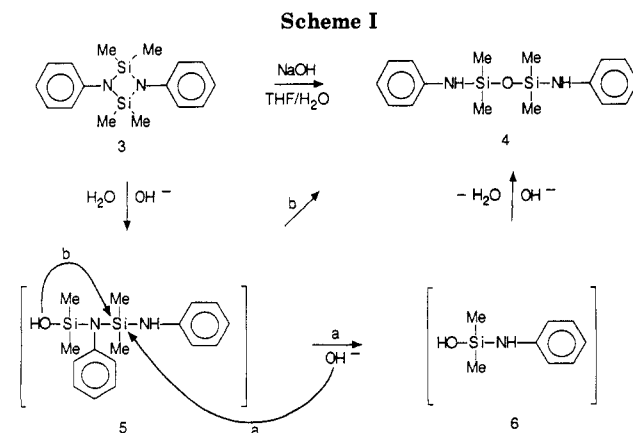The relatively unhindered N,N'-diphenyltetramethylcyclodisilazane, $(Me_2SiNPh)_2$, readily undergoes hydrolysis in the presence of catalytic amounts of acid or base. Under basic conditions, an intermediate diaminodisiloxane, $[Me_2Si(NHPh)]_2O$, can be isolated. Under acidic conditions, hydrolysis rates are proportional to the strength of the acid used with the exception of tetrafluoroboric acid which exhibits an accelerated hydrolysis rate. The more sterically congested hexaphenylcyclodisilazane, $(Ph_2SiNPh)_2$, is resistant to acid hydrolysis, but it is readily hydrolyzed in the presence of base. Hydrolysis of the hexaphenyl derivative in the presence of fluoride ion gives rise to several fluorine-containing products such as $(Ph_2SiF)_2NPh$.

The thermally stable[1] cyclodisilazane ring 1 is a potentially useful structure in small-ring chemistry. These planar, relatively unstrained systems[2] were incorporated into the backbone of linear polymer chains to enhance their thermal stability[3] and into silazane polymer networks to increase yields of silicon nitride and silicon carbide ceramics.[4] Despite their attractive thermal characteristics, only a handful of examples are cited that use these cyclic units in polymeric materials. This is in part because of the hydrolytic instability of the silicon–nitrogen bond.

1

Several studies were published on the hydrolysis of silylamines, linear silazanes,[5] and N-silyl-substituted cyclodisilazanes 2. In the latter, when R = methyl, reactions of 2 with alcohols,[6] water,[7] acetic acid,[8] and hydrogen

(1) (a) Breed, L. W.; Elliott, R. L.; Ferris, A. F. J. Org. Chem. 1962, 27, 1114. (b) Fink, W. Helv. Chim. Acta 1969, 52, 1841.

(2) (a) Parkanyi, L.; Bihatsi, L.; Hencsei, P.; Szollosy, A. J. Organomet. Chem. 1987, 321, 7. (b) Szollosy, A.; Parkanyi, L.; Bihatsi, L.; Hencsei, P. Ibid. 1983, 251, 159. (c) Gergo, E.; Schultz, G.; Hargittai, I. Ibid. 1985, 292, 343. (d) Parkanyi, L.; Argay, G.; Hencsei, P.; Nagy, J. Ibid. 1976, 116, 299. (e) Parkanyi, L.; Szollosy, A.; Bihatsi, L.; Hencsei, P.; Nagy, J. Ibid. 1983, 256, 235. (f) Bihatsi, L.; Hencsei, P.; Parkanyi, L. Ibid. 1981, 219, 145. (g) Parkanyi, L.; Dunaj-Jurco, D.; Bihatsi, L.; Hencsei, P. Cryst. Struct. Commun. 1980, 9, 1049.

(3) Fink, W. J. Paint Technol. 1970, 42, 220 and references therein.

(4) (a) Seyferth, D.; Wiseman, G. H. U.S. Patent 4 482 669. (b) Seyferth, D.; Wiseman, G. H. J. Am. Ceram. Soc. 1984, 67, C132.

(5) Bazant, V.; Chvalovsky, V.; Rathousky, J. Organosilicon Compounds; Academic: New York, 1965; Vol. I, pp 76–88 and references therein.

(6) Varezhkin, Y. M.; Morgunova, M. M.; Zhinkin, D. Y. Zh. Obshch. Khim. 1980, 50, 2009 (Engl. Transl.).

(7) (a) Varezhkin, Y. M.; Morgunova, M. M.; Zhinkin, D. Y. Zh. Obshch. Khim. 1977, 47, 1410 (Engl. Transl.). (b) Varezhkin, Y. M.; Zhinkin, D. Y.; Morgunova, M. M.; Bochkarev, V. N. Ibid. 1974, 45, 2410 (Engl. Transl.).

Scheme I

chloride[9] initially resulted in cleavage of the exocyclic Si–N bond (eq 1). Further reaction with the cyclodisilazane ring

$$(1)$$
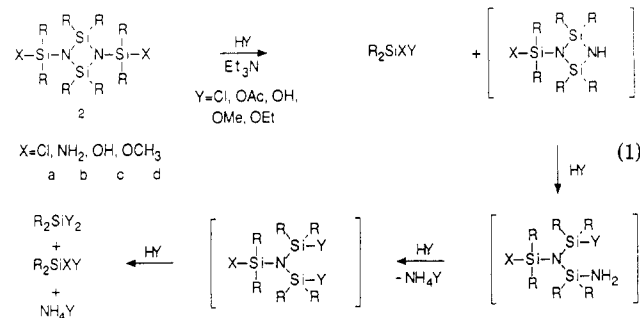
then occurred to give the products shown. The amount of protic reagent (stoichiometric or excess) and the presence or absence of a proton acceptor (Et₃N) dictated the

(8) Varezhkin, Y. M.; Morgunova, M. M.; Zhinkin, D. Y. Zh. Obshch. Khim. 1981, 51, 347 (Engl. Transl.).

(9) Varezhkin, Y. M.; Morgunova, M. M.; Zhinkin, D. Y. Zh. Obshch. Khim. 1980, 50, 1100 (Engl. Transl.).